Verification of a Linear Relation between IR Extinction, Absorption and Liquid Water Content of Fogs

R. G. PINNICK

U.S. Army Atmospheric Sciences Laboratory, White Sands Missile Range, NM 88002

S. G. JENNINGS[1]

Department of Pure and Applied Physics, University of Manchester Institute of Science and Technology, Manchester, England

PETR CHÝLEK

Center for Earth and Planetary Physics, Harvard University, Cambridge, MA 02138

H. J. AUVERMANN

Physical Sciences Laboratory, New Mexico State University, Las Cruces, NM 88003

(Manuscript received 15 December 1978, in final form 3 April 1979)

ABSTRACT

A linear relationship, independent of the form of the size-distribution, between extinction at wavelengths around $\lambda = 11$ μm, absorption around $\lambda = 3.8$ and 9.5 μm, and liquid water content of atmospheric fogs has been verified using 341 droplet size distribution measurements made under a variety of meteorological conditions. The results suggest that integrated liquid water content along a path in fog can be determined from measurement of CO_2 laser ($\lambda = 10.6$ μm) transmission along the path, and that liquid water content at a particular point in fog can be inferred from *in situ* measurement of fog-droplet absorption with a deuterium fluoride laser ($\lambda = 3.8$ μm) or a suitably tuned CO_2 laser ($\lambda = 9.5$ μm) spectrophone.

1. Introduction

It has been recently shown (Chýlek, 1978) that a linear relationship, independent of the form of the size distribution, should exist between the infrared extinction around $\lambda = 11$ μm and the liquid water content of fogs. The relation can be written in the form

$$\sigma_e = \frac{3\pi c}{2\rho\lambda} W, \tag{1}$$

where σ_e is the volume extinction coefficient measured at the wavelength λ, W the liquid water content, ρ the density of water, and the coefficient c is equal to the slope of a straight line that approximates the extinction efficiency curve $Q_e(x,\lambda)$ by

$$Q_e(x,\lambda) \approx c(\lambda)x, \tag{2}$$

where the size parameter x is defined by the ratio of the particle circumference to the wavelength. An approximate value of the coefficient $c(\lambda)$ at $\lambda = 11$ μm is $c \approx 0.31$. The conditions under which the approximation (2) are valid and the derivation of the relation (1) have been discussed elsewhere (Chýlek, 1978).

In this paper we verify the validity of relation (1) by calculating the volume extinction coefficient σ_e and the liquid water content W for 341 different fog droplet size distributions (Garland, 1971; Kumai, 1973; Garland *et al.*, 1973; Kunkel, 1971; Roach *et al.*, 1976; Pinnick *et al.*, 1978) measured under various meteorological situations.

We also show that a linear relationship, similar to (1), exists between the infrared absorption coefficient in the spectral regime $\lambda = 3.5$–5.3 μm, 8–10 μm, and the liquid water content of fogs. Thus for example, the absorption coefficient of fogs at $\lambda = 3.8$ μm is uniquely related to their extinction and absorption at $\lambda = 10$ μm.

2. Selected fog size distributions

Relatively few reliable measurements of fog droplet size distributions have been made, particu-

[1] Visiting U.S. Army Atmospheric Sciences Laboratory.

0022-4928/79/081577-10$06.50

larly for which numerical data are available. The fog measurements used here we judge to be reliable and were chosen to represent a wide range of fog conditions ranging from maritime and continental advection fogs [Kumai, 1973; Kunkel, 1971; and part of Garland's (1971) work] to inland radiation fogs (Garland, 1971; Garland *et al.*, 1973; Roach *et al.*, 1976; Pinnick *et al.*, 1978). The early work on evolving fogs near the Atlantic Ocean in France and stable inland fog and haze near Paris by Arnulf *et al.* (1957) was not used because it was not possible to obtain true droplet distributions from their figures. Arnulf *et al.* (1957) captured droplets on spider threads (for which the capture coefficient depends on droplet size) but gives only the uncorrected droplet distribution data. Results of the pioneering work of May (1961) using a specially designed two-stage impactor were not used since the numerical data are no longer available (May, private communication, 1978). Measurements of valley fog drop sizes obtained by exposing gelatin-coated slides to a stream of foggy air by Pilié *et al.* (1975) were deemed not credible since the distributions were normalized to simultaneous measurements of extinction coefficient derived by a transmissometer. Fog drop measurements made with a light-scattering counter by Eldridge (1961) were not utilized since we suspect errors in his measurements due to non-isokinetic sampling. The inlet of his counter was only 1 cm in diameter and became wet during the sampling process. In addition, some unexplained differences were caused by a dilution apparatus Eldridge used for high droplet concentration conditions.

Three different sampling techniques were employed to obtain the fog size distributions utilized in this study: impaction, holographic and light scattering.

Garland (1971), Garland *et al.* (1973) and Roach *et al.* (1976) used a modified two-stage Casella impactor designed by May (1961) mounted horizontally in a wind tunnel to provide isokinetic sampling. Corrections to the collection efficiency based on the penetration curves of the impactor (May, 1945) were applied to the raw data. This device is sensitive to droplets of 0.3–72 μm radius.

Kumai (1973) also used a two-stage impactor to measure advection fog droplets formed over the Arctic Ocean at Point Barrow, Alaska, together with a gelatin-coated glass slide collection plate whose collection efficiency was calculable as a function of wind velocity. Also, imprint-droplet correction factors were applied to obtain true sizes. The combined methods yielded drop size concentration from 2.2–64 μm radius.

In general, the primary deficiency of the impaction technique, besides requiring laborious data reduction, is the uncertainty in number concentration determination for near-micrometer and submicrometer size droplets. In addition, the size limit of detectability is about 0.3 μm radius using conventional microscopy techniques.

A laser hologram technique was employed by Kunkel (1971) to measure droplets in advection fog propagating inland during nighttime at Otis Air Force Base, Massachusetts. The hologram camera was capable of sampling volumes of 4.5 cm^3 at a rate of five samples per minute, in a near-isokinetic fashion, and with minimal disturbance to the droplets. Droplets with radius 2–40 μm were detected. Because of the small number of droplets (normally <50) in the distributions reported by Kunkel, we have averaged all 17 of the reported droplet distributions together, which in any case represents only a 3-min interval, to obtain a single distribution.

Finally, we have used measurements by Pinnick *et al.* (1978) of radiation fog and haze made during wintertime in West Germany with a commercially available light-scattering counter (the "Knollenberg" Classical Scattering Aerosol Spectrometer manufactured by Particle Measurement Systems, Boulder, Colorado). This device works on the principle that as aerosol flows through an illuminated volume, light scattered by single droplets into a particular solid angle is measured and used to determine particle size by making pulse-height analyses of the response pulses. Determination of droplet size from the response is indirect because of the dependence of the response on factors other than droplet size, viz., droplet refractive index and the lens geometry of the optical system. Particular attention was given to the calibration of this instrument using monodisperse particles of different size and refractive index. The manufacturer's advertised calibration was not used. Rather, droplet size distributions were determined by redefining the size pulse-height channels as described in detail by Pinnick *et al.* (1978). This counter is sensitive to water droplets with radii 0.23–16 μm.

Altogether, 341 different size distributions were used to check the validity of Eq. (1) in the atmospheric window around $\lambda = 11$ μm; 25 fog distributions were taken from Garland (1971) and Roach *et al.* (1976), 6 from Garland *et al.* (1973), 20 from Kumai (1973), 1 from Kunkel (1971), and 289 fog and haze distributions from Pinnick *et al.* (1978).

3. Numerical results for fog extinction

Using a Mie scattering program and index of refraction of water as given by Hale and Querry (1973), we have calculated the volume extinction coefficient

$$\sigma_e(\lambda) = \pi \int r^2 Q_e(\lambda, r) n(r) dr \qquad (3)$$

and the liquid water content

$$W = \tfrac{4}{3}\pi\rho \int r^3 n(r) dr \qquad (4)$$

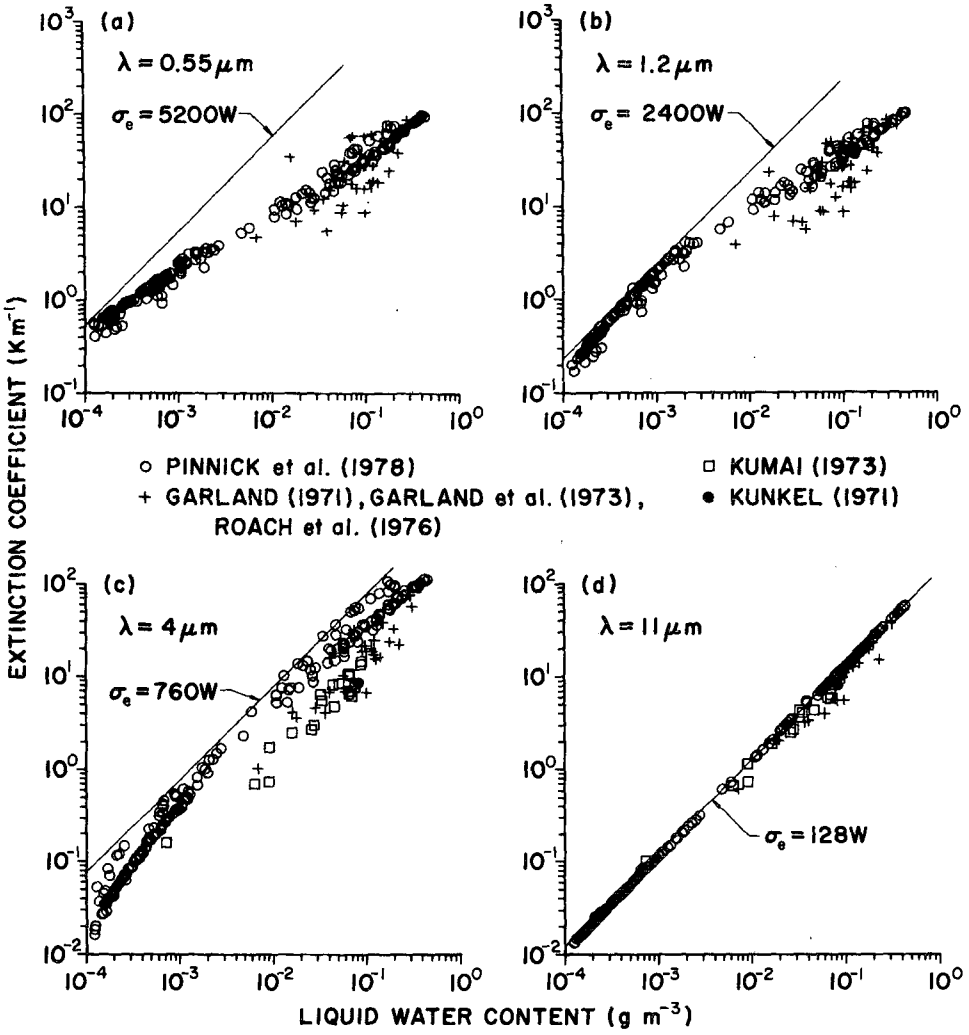

FIG. 1. Variation of extinction coefficient with liquid water content in atmospheric fog and haze for 341 size distribution measurements made at different geographic locales and under a variety of meteorological conditions. In the infrared spectral region around $\lambda = 11$ μm (d) there exists a linear, size-distribution-independent relation between the volume extinction coefficient $\sigma_e(\text{km}^{-1})$ and the liquid water content W (g m $^{-3}$) of the form of Eq. (1). Consequently, the results of all measurements are close to a straight line. The predicted relation between extinction σ_e and liquid water content W according to Eq. (1) is shown by the straight line. On the other hand at $\lambda = 0.55$ μm (a), the $Q_e = cx$ approximation is not satisfied and no unambiguous relation between the extinction and liquid water content exists. The large spread of the points in the graph shows that the extinction coefficient is a function of the size distribution as well as of the liquid water content. As the wavelength is increased to $\lambda = 1.2$ μm (b) and $\lambda = 4$ μm (c) the $Q_e = cx$ approximation is satisfied for larger droplets and the relation (1) shown by the straight lines is becoming a more realistic approximation for hazes and fogs.

for the previously mentioned 341 fog and haze size distributions $n(r)$ at several different wavelengths λ. The numerical integrations were performed only over the range of particle radii measured for each size distribution, under the assumption that the differential size distribution $n(r)$ is constant within each measured particle size channel. In other words, there was no extension of the measured distributions to larger or smaller particle sizes and no smoothing of the measured distributions. The results at $\lambda = 0.55$, 1.2, 4 and 11 μm, together with the $Q_e = cx$ approximation [Eq. (1)] are shown in Fig. 1. We have not included the Kumai (1973) or Kunkel (1971) results at $\lambda = 0.55$ μm, 1.2 μm since we suspect the contribution of particles with $r \lesssim 2$ μm (which neither Kumai nor Kunkel measured) to extinction at these wavelengths might be excessive.

At $\lambda = 11$ μm the $Q_e = cx$ approximation is a good approximation for all size distributions except those with a large number of droplets with radii $r > 14$ μm (Chýlek, 1978). Some fog size distributions used in our calculations contained droplets

with $r > 14$ μm; however, their contribution generally did not dominate either the extinction σ_e or the liquid water content W. Consequently, we expect that the linear relationship (1) between the volume extinction coefficient σ_e and the liquid water content W will be reasonably well satisfied at $\lambda = 11$ μm. Results of numerical calculations confirming the validity of Eq. (1) at $\lambda = 11$ μm are shown in Fig. 1d.

On the other hand at $\lambda = 0.55$ μm the approximation $Q_e = cx$ is valid only for water droplets with $r \leq 0.5$ μm (Chýlek, 1978). Since most haze and all fog droplet size distributions are dominated by droplets with $r > 0.5$ μm, the $Q_e = cx$ approximation is not valid in this case and, consequently, no size-distribution-independent relation between the extinction and liquid water content should exist at $\lambda = 0.55$ μm. The numerical results based on the measured distributions compared to the Eq. (1) approximation in Fig. 1a confirm this conclusion. Further, the approximation grossly overestimates extinction for most of the distributions.

As we change the wavelength from $\lambda = 0.55$ μm to longer wavelengths, the $Q_e = cx$ approximation is satisfied for larger droplet radii r. Consequently, with increasing wavelength the relation given by Eq. (1) is becoming a more realistic approximation for hazes and for fogs. This trend can be seen from Figs. 1b–1c, showing the numerical calculations and the Eq. (1) approximation at $\lambda = 1.2$ and 4 μm. We note that with increasing λ the relation (1) better approximates the exact numerical results and finally at $\lambda = 11$ μm (Fig. 1d) the volume extinction coefficient becomes independent of the size distribution $n(r)$, and the relation (1) agrees within a factor 2 with the numerical results for all distributions.

Closer inspection of the results in Fig. 1d shows noticeably better agreement between the Mie numerical results and the relation (1) for the size distributions of Pinnick *et al.* (1978). The reason very likely has to do with the fact that the size distribution measurements of Pinnick *et al.* are only for droplets with radii up to $r \doteq 16$ μm, whereas the Garland (1971), Garland *et al.* (1973) and Roach *et al.* (1976) measurements are for droplets with radii up to $r = 72$ μm; the Kumai (1973) measurements are for droplets with radii up to $r = 64$ μm; and the Kunkel (1971) measurement is for droplets with radii up to $r = 40$ μm. Since the maximum radius condition for the $Q_e = cx$ approximation leading to relation (1) is for $r_m = 14$ μm at $\lambda = 11$ μm, none of the Pinnick *et al.* distributions can strongly violate this condition as no particles with $r > 16$ μm were measured. Thus, the better agreement of the numerical results for the Pinnick *et al.* distributions with the relation (1) at $\lambda = 11$ μm [and also at $\lambda = 4$ μm (see Fig. 1c)] may be in part a consequence of their inability to measure droplets with $r > 16$ μm.

Another qualification concerning the results in Fig. 1 bears on our assumption that all fog and haze particles consist of homogeneous water droplets and have complex refractive indexes of water. Haze particles in particular may contain a significant volume fraction of contaminants such as sea salt or ammonium sulfate. The crucial question here is to what degree is the particle refractive index affected by such contaminants? We know in the case of fog that its formation requires atmospheric relative humidity RH to be near 100%. We also know that for the haze data appearing in Fig. 1 the relative humidity was close to 100% (Pinnick *et al.*, 1978). Hänel (1976) and Hänel and Bullrich (1978) have studied the effect of relative humidity variations on mean complex refractive indexes of maritime and urban aerosols. Hänel (1976) found that for RH $\geq$ 95% the real and imaginary parts of the complex refractive index n_{re} and n_{im} at $\lambda = 0.55$ μm have values $1.33 \leq n_{re} \leq 1.36$, $0 \leq n_{im} \leq 0.006$. Examination of Mie efficiency factors $Q_e(m,x)$ for refractive indexes in this range shows our assumption that $m = 1.33-0i$ in Mie calculations of extinction according to (3) and the $Q_e = cx$ approximation (1) is a good one. At wavelengths $>\lambda = 0.55$ μm we find from Hänel and Bullrich's formulas for values of RH >95% that both maritime and urban aerosol mean refractive indexes are again not markedly different from those of water. For example, at $\lambda = 11$ μm we predict from Hänel and Bullrich's formulas that the real and imaginary parts of the complex index are $1.153 \leq n_{re} \leq 1.207$, $0.0968 \leq n_{im} \leq 0.109$, compared to $m = 1.153-0.0968i$ for pure water. The effect of these refractive index variations in Mie calculations of extinction coefficient according to (3) and (1) are estimated to be not more than 10%. For fog, an additional argument can be made to support our assumption that the particle refractive indexes can be approximated by those of pure water. The argument is that the liquid mass content of fogs is on the order of 0.005 g m^{-3} or greater, and thus the volume fraction of any contaminant in fog droplets must necessarily be small so that the refractive indexes must be close to those of water.

In order to examine more closely the fog results in Fig. 1 in terms of fog type we have chosen to restrict our attention to the data of Garland (1971), Garland *et al.* (1973) and Roach *et al.* (1976). The reasons are twofold: first, these measurements were made during fogs occurring under distinctly different meteorological conditions. Altogether, 37 different fogs were measured during a five-year period under the gamut of meteorological conditions found in England. Second, measurements were made for a

sufficiently broad range of particle sizes (0.3 μm $< r <$ 72 μm) that errors in extinction and liquid water content due to the presence of larger and smaller droplets are estimated to be small. Of the 37 measured distributions, three were not used due to nonavailability of the raw data, three because of the presence of ice crystals in the samples, and five were not used because fog type was not specified.

We have divided the Garland and Roach *et al.* fog data, which already appear in Fig. 1, into two classes: radiation fog and advection fog. We have been cautioned (Garland, private communication, 1978) that although the radiation fogs clearly formed *in situ* by radiation cooling, some fogs classified as advection type may have been mature radiation fogs transported by the wind from a distant area of formation. In any case, the data are replotted according to this classification in Fig. 2 (λ = 0.55 μm) and Fig. 3 (λ = 11 μm). At λ = 0.55 μm it is evident radiation fogs are generally more effective scatterers, and hence more effective in reducing visibility, than advection fogs with the same liquid water content. To understand the reason for this result, we have picked a radiation fog (Fig. 2, solid circle) and an advection fog (Fig. 2, solid square) measurement with about the same liquid water content, and have plotted their differential extinction coefficients at λ = 0.55 μm vs particle radius in Fig. 4. Because the plots are made on a linear scales, the areas under the curves are a measure of the corresponding extinction coefficients. Thus the radiation fog extinction coefficient (35 km^{-1}) is more than twice the advection fog extinction coefficient (15.8 km^{-1}). For the radiation fog, small droplets, say, $r \leq 3$ μm, are very numerous and contribute 60% of the extinction without making a significant contribution to liquid water content. On the other hand, for advection fog, a broader size distribution is found and these smaller particles contribute only 6% of the extinction at λ = 0.55 μm. Both the radiation and the advection fog size distributions strongly violate the maximum radius condition allowed in the $Q_e = cx$ approximation (r_m = 0.5 μm at λ = 0.55 μm), so there is no reason to expect a unique relation between extinction at λ = 0.55 μm and liquid water content.

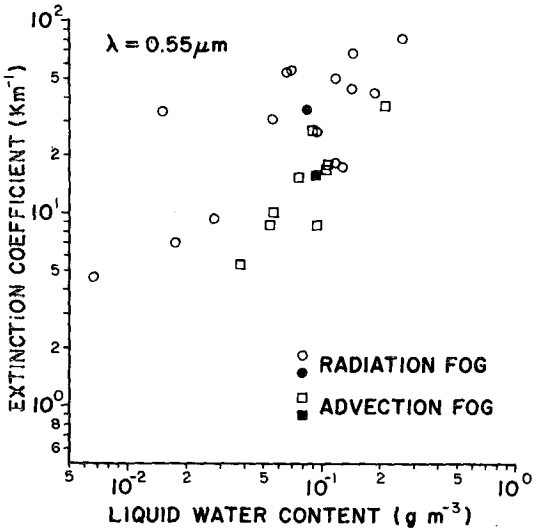

FIG. 2. As in Fig. 1a except that only the fog data of Garland (1971), Garland *et al.* (1973) and Roach *et al.* (1976) are shown. The extinction and liquid water contents calculated from the 26 measured size distributions are divided according to radiation (circles) or advection (squares) fog. We see from the figure that radiation fogs are generally more effective scatterers than advection fogs with the same liquid water content because they contain more droplets in the Mie resonance region that contribute a significant part of the extinction but contribute only a marginal amount to the liquid water content.

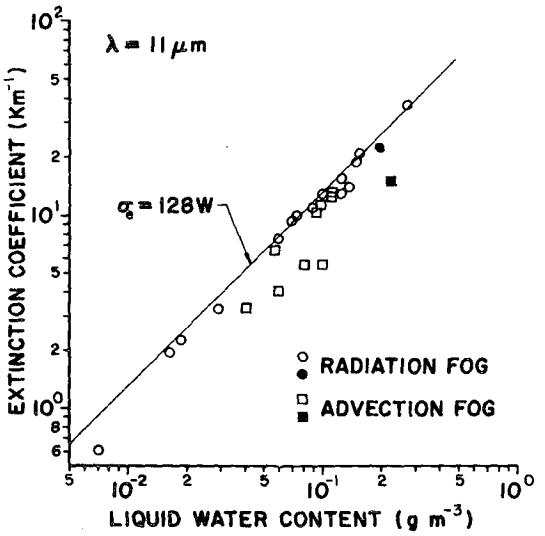

FIG. 3. As in Fig. 2 except for λ = 11 μm. The predicted relation between extinction and liquid water content given by Eq. (1) is shown by the straight line. Because the $Q_e = cx$ approximation is generally better satisfied for radiation fogs, those points fall closer to the straight line prediction.

At λ = 11 μm (Fig. 3), although the $Q_e = cx$ approximation is within a factor of about 2 for both radiation and advection fog results, the approximation is generally in better agreement with the radiation fog results. The explanation is that the $Q_e = cx$ approximation is only strictly valid providing fog droplets have $r \gtrsim 14$ μm (Chýlek, 1978) and radiation fogs better satisfy this condition than do advection fogs. The degree to which this maximum radius condition is violated can be determined for two fog examples from Fig. 5. Shown is the differential extinction coefficient at λ = 11 μm for a radiation fog (Fig. 3, solid circle) and an advection fog (Fig. 3,

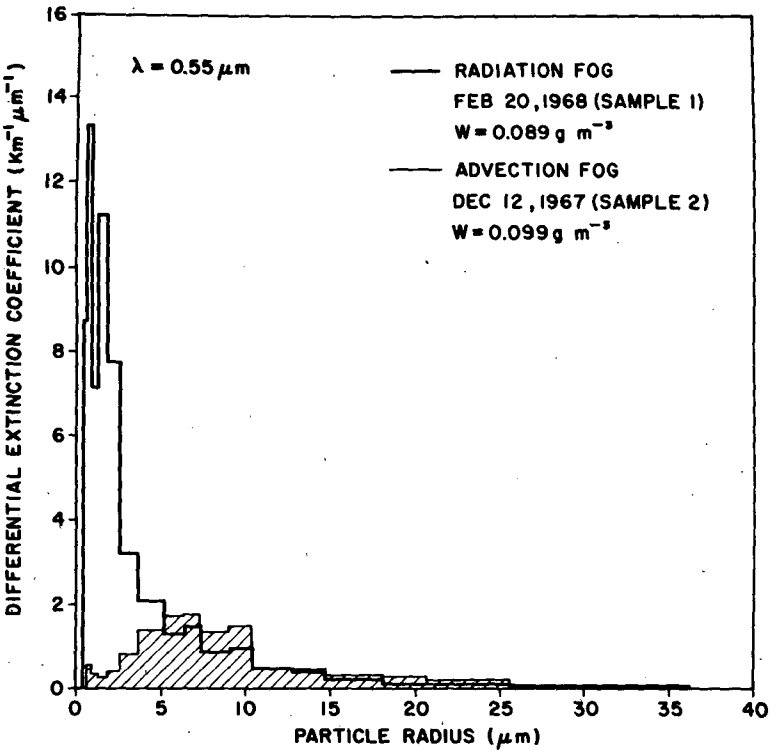

FIG. 4. Differential extinction coefficients at $\lambda = 0.55$ μm versus droplet radius for a radiation fog (solid circle in Fig. 2) and an advection fog (solid square in Fig. 2) with about the same liquid water content. The areas under the curves are a measure of the total extinction coefficients (35 km^{-1} for the radiation fog versus 15.8 km^{-1} for the advection fog). For the radiation fog, 60% of the extinction is contributed by droplets having $r \leq 3$ μm, compared to only 6% for the advection fog.

solid square) again having about the same liquid water content. For the radiation fog 69% of the extinction arises from droplets with radii less than the maximum value $r_m = 14$ μm, while for the advection fog this value drops to 33%. A survey of all the differential extinction coefficient versus particle radius graphs similar to those shown in Fig. 5 for the radiation fogs of Garland (1971), Garland *et al.* (1973) and Roach *et al.* (1976) in Fig. 3 show that in all cases extinction at $\lambda = 11$ μm is dominated by droplets with $r \leq 14$ μm. On the other hand, a survey of the differential extinction coefficient graphs for the advection fogs presented in Fig. 3, and also the advection fogs of Kumai (1973), show that for about one-half of the distributions, extinction at $\lambda = 11$ μm is dominated by droplets with $r > 14$ μm. Since the extinction efficiency factor for these larger particles is overestimated by the $Q_e = cx$ approximation (see Fig. 3 of Chýlek, 1978), the numerical calculation of the extinction for these advection fogs fall below the Eq. (1) prediction in Fig. 3. For the remaining half of the advection fogs, droplets with $r \leq 14$ μm dominate extinction and the points fall within 20% of the Eq. (1) prediction. Thus, while droplets with $r \leq 14$ μm dominate extinction at $\lambda = 11$ μm for radiation fog, this is not always the case for advection fog, where the presence of larger droplets partially destroys the size distribution independent linear relation (1).

4. $Q_a = c'x$ approximation for absorption

Realizing that the $Q_e = cx$ approximation works reasonably well for fog at $\lambda \approx 11$ μm, and for haze at shorter wavelengths, we checked to see if a similar approximation for fog droplet absorption might hold in the $\lambda = 3$–5 μm and $\lambda = 8$–12 μm atmospheric window spectral regions.

The absorption coefficient σ_a for a polydispersion of droplets described by the size distribution $n(r)$ is given by

$$\sigma_a = \int \pi r^2 Q_a(m,x) n(r) dr, \qquad (5)$$

where $Q_a(m,x)$ is the Mie efficiency factor for absorption for a water droplet with refractive index $m(\lambda)$ and size parameter $x = 2\pi r/\lambda$. Plots of the efficiency factor for absorption Q_a vs x for $\lambda = 3.8$,

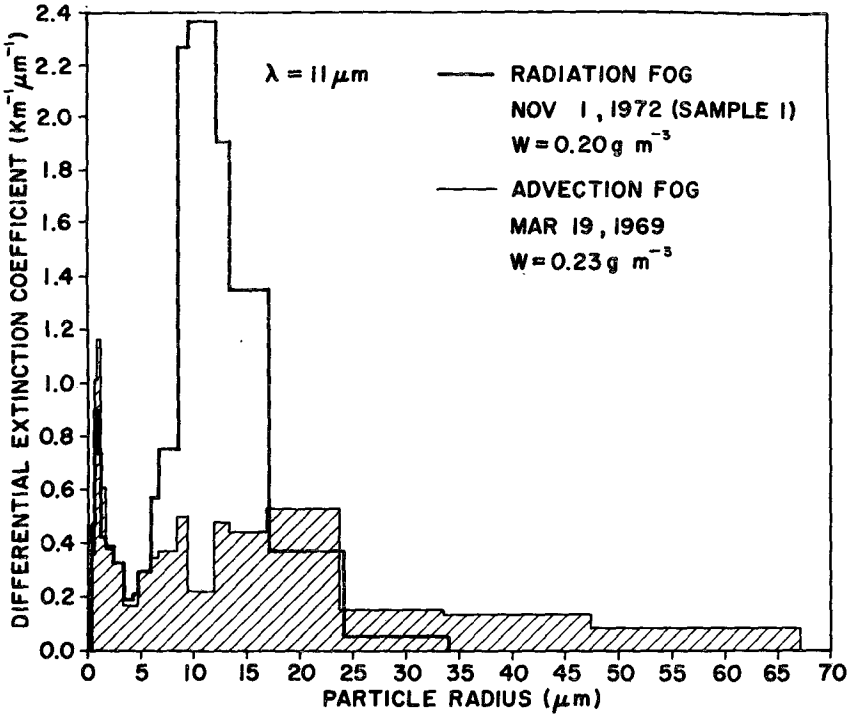

FIG. 5. Differential extinction coefficients at $\lambda = 11$ μm versus droplet radius for a radiation fog (solid circle in Fig. 3) and an advection fog (solid square in Fig. 3) with about the same liquid water content. The total extinction for the radiation fog is 22.6 km^{-1} compared to 15.0 km^{-1} for the advection fog. The fraction of extinction contributed by droplets with $r \leq 14$ μm (the maximum value allowed in the $Q_e = cx$ approximation) is 69% for the radiation fog, decreasing to 33% for the advection fog. Thus the prediction between extinction (at $\lambda = 11$ μm) and liquid water content [given by Eq. (1) and shown in Fig. 3] is a better approximation for radiation fogs than for advection fogs.

9.5 μm are shown in Figs. 6 and 7. Again we find, as Chýlek (1978) found for extinction, that Q_a can be well approximated by $Q_a(x,\lambda) \approx c'(\lambda)x$, providing $x \leq x_m$.

Using this linear approximation for Q_a in (5) gives

$$\sigma_a = \frac{3\pi c'}{2\lambda\rho} \int \frac{4\pi r^3}{3} n(r)dr. \tag{6}$$

Thus, explicit dependence on the size distribution disappears and leads to the absorption coefficient being linearly related to liquid water content W according to

$$\sigma_a = \frac{3\pi c'}{2\lambda\rho} W. \tag{7}$$

As in the case of extinction the restriction that $x \leq x_m$ need not be strictly satisfied, but water droplets with radii greater than the value $r_m = \lambda x_m/2\pi$ must not contribute excessively to either absorption or liquid water content. Numerical values of the maximum radii r_m at various wavelengths λ as well as the slope c' of a straight line approximating Q_a for $x \leq x_m$, are given in Table 1.

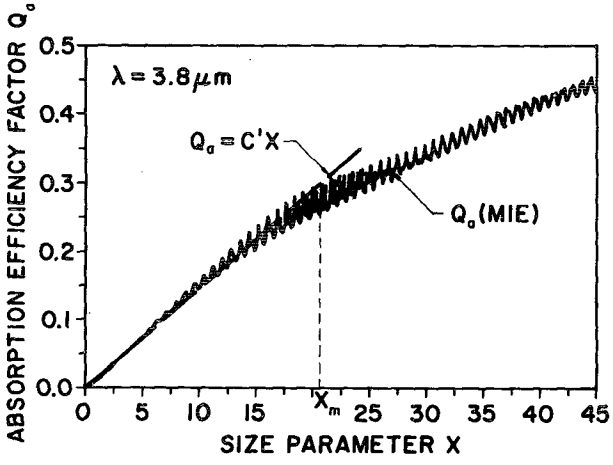

FIG. 6. The efficiency factor for absorption Q_a for water versus droplet size parameter x at a wavelength $\lambda = 3.8$ μm (index of refraction $m = 1.364-0.0034i$). The efficiency factor can be approximated by a straight line $Q_a = c'x$ providing $x \leq x_m$. The approximation overestimates the exact value of Q_a for some size parameters, but underestimates it for others. These two errors tend to cancel leading to the absorption coefficient being linearly related to liquid water content according to equation (7).

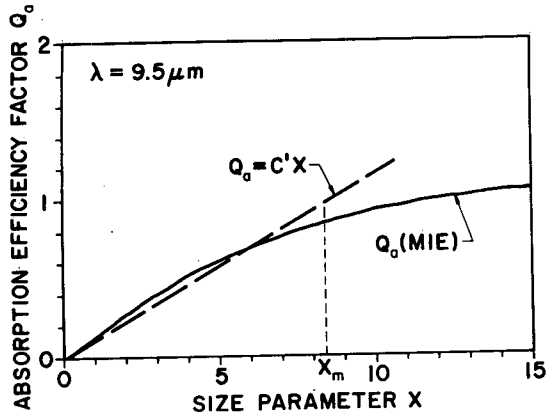

FIG. 7. As in Fig. 6 except for $\lambda = 9.5$ μm (index of refraction of water $m = 1.243-0.0443i$). The efficiency factor for absorption can again be approximated by a straight line $Q_a = c'x$ providing $x \leq x_m$.

Also given are values of the quantity $3\pi c'/2\lambda\rho$ which if multiplied by the liquid water content give the absorption coefficient. In order that these predicted relationships (and maximum radius conditions) between droplet absorption and liquid water content may be compared to the corresponding results for extinction, the values of x_m, r_m, etc., for the $Q_e = cx$ approximation (Chýlek, 1978) for extinction also appear in Table 1. The values of x_m, r_m and c for extinction are sometimes slightly different from those of Chýlek (1978) since there is some leeway in the subjective procedure for approximating the efficiency factor $Q_e(x)$ by a linear function of size parameter x. We see from the table that the limiting radius r_m depends strongly on wavelength and is in general markedly different for absorption and extinction at a particular wavelength. An exception is at $\lambda = 9.5$ μm, where the limiting radii are $r_m = 13$ μm for absorption as compared to $r_m = 12.5$ μm for extinction. Thus for fog droplet distributions that have radii $r < 12.5$ μm (i.e., most radiation fogs) we can predict from Table 1 that absorption contributes 29% of the extinction at $\lambda = 9.5$ μm, independent of the form of the droplet size distribution. However, there is obviously no unique relation between fog absorption and extinction for all wavelengths.

Since we have verified the $Q_e = cx$ approximation for extinction at $\lambda = 11$ μm, which requires that droplets have maximum radius $r_m = 14$ μm, is adequate for atmospheric fog, we suspect the $Q_a = c'x$ approximation for absorption is adequate for fog at selected wavelengths also having $r_m \approx 14$ μm. From Table 1 we see that wavelengths $\lambda = 3.8$, 4, 5.3 and 9.5 μm either satisfy or nearly satisfy this criterion. Therefore, we might expect a linear relation between fog absorption and fog liquid water content according to (7), independent of the droplet size distribution, for these particular wavelengths.

To check this contention we have calculated the volume absorption coefficient $\sigma_a(\lambda)$ using a Mie scattering program according to Eq. (5) for the previously mentioned 341 fog and haze size distributions at several different wavelengths. As in the extinction calculations we have assumed particle refractive indexes of water, and have thus neglected refractive index differences that might be caused by the presence of contaminants such as sea salt and ammonium sulfate. The results at $\lambda = 3.8$, 9.5 μm plotted as a function of fog liquid water content together with the $Q_a = c'x$ approximation (7) are shown in Figs. 8 and 9. We see that although the numerical results are slightly better approximated at $\lambda = 3.8$ μm as compared to $\lambda = 9.5$ μm, at both wavelengths the linear relation (7) is within a factor 2.5 of the numerical results for all 341 fog and haze size distributions. Examination of results at numerous other infrared wavelengths show that even though the maximum radius condition is sometimes violated, for $\lambda = 3.5$–5.3 μm, 8–10 μm all numerical results for the 341 fog distributions are within a factor 2.5 of the predictions between absorption and liquid water content given by relation (7) and listed in Table 1, and in most cases the agreement is within a factor 2. However, at wavelengths $\lambda = 10.5$–12 μm, the numerical results differ by as much as a factor 4 from the linear relation (7).

Previously, Platt (1976) found an approximate linear relation between the absorption coefficient

TABLE 1. At a given wavelength λ the efficiency factor for absorption Q_a (and extinction Q_e) can be approximated by a straight line $Q_a = c'x$($Q_e = cx$) for size parameters $x \leq x_m$. The values of x_m and c' (and c) are determined from the efficiency curves (see, e.g., Figs. 6 and 7). If we know the maximum radius r_m of droplets in a given size distribution, the table gives the wavelength λ at which a linear relationship between absorption (or extinction) and liquid water content exists, and the appropriate value of the parameter c' (or c). The value of the quantity $3\pi c'/2\lambda\rho$ (or $3\pi c/2\lambda\rho$) multiplied by the liquid water content W gives the absorption coefficient σ_a (or extinction coefficient σ_e).

	Absorption				Extinction			
λ (μm)	x_m	r_m (μm)	c'	$3\pi c'/2\lambda\rho$ (cm^2 g^{-1})	x_m	r_m (μm)	c	$3\pi c/2\lambda\rho$ (cm^2 g^{-1})
3.0	2.3	1.1	0.58	9.1×10^3	3.2	1.5	0.85	13.3×10^3
3.5	14	8.0	0.037	0.50×10^3	5.9	3.3	0.72	9.6×10^3
3.8	21	13	0.015	0.18×10^3	6.5	4.0	0.66	8.2×10^3
4.0	22	14	0.018	0.22×10^3	6.7	4.3	0.64	7.6×10^3
4.5	14	10	0.047	0.49×10^3	7.0	5.0	0.59	6.1×10^3
5.0	14	11	0.044	0.41×10^3	7.2	5.8	0.56	5.3×10^3
5.3	16	14	0.035	0.31×10^3	7.5	6.3	0.56	5.0×10^3
8.0	7.6	9.7	0.10	0.61×10^3	7.3	9.3	0.51	3.0×10^3
8.5	8.2	11	0.11	0.60×10^3	7.9	10.7	0.45	2.5×10^3
9.0	8.0	12	0.11	0.57×10^3	8.0	11.5	0.44	2.3×10^3
9.5	8.4	13	0.12	0.58×10^3	8.2	12.5	0.41	2.0×10^3
10.0	7.0	11	0.13	0.60×10^3	8.8	14	0.38	1.8×10^3
10.5	6.0	10	0.16	0.70×10^3	8.6	14	0.33	1.5×10^3
11.0	4.1	7.2	0.21	0.93×10^3	8.1	14	0.31	1.3×10^3
11.5	3.1	5.7	0.30	1.26×10^3	5.0	9.1	0.37	1.5×10^3
12.0	2.3	4.5	0.42	1.65×10^3	4.9	9.3	0.44	1.7×10^3
12.5	1.9	3.7	0.58	2.2×10^3	3.7	7.3	0.58	2.2×10^3

σ_a at $\lambda = 11$ μm and liquid water content W of non-precipitating stratocumulus clouds. Platt performed Mie calculations on 25 measured cloud droplet distributions, plotted the values of σ_a at $\lambda = 11$ μm vs W, did a least-squares fit through the resulting data points and obtained $\sigma_a = 76.5\ W$, comparing modestly well with our Eq. (7) prediction from Table 1 of $\sigma_a = 93\ W$, where the absorption is in km^{-1} and the liquid water content in g m^{-3}. The reason for our overprediction of the absorption is that a significant number of droplets in Platt's distributions have radii >7.2 μm, the maximum value allowable in the $Q_a = c'x$ approximation at $\lambda = 11$ μm. Had Platt chosen a slightly shorter wavelength, say, $\lambda = 9.5$ μm, he would have found an even better correlation of absorption and liquid water content, as well as better agreement with our linear prediction (7), since the maximum radius restriction is more nearly satisfied for clouds at the shorter wavelength.

5. Application of extinction—absorption-liquid water content relationships

The unique, linear, size-distribution-independent relationship between extinction at $\lambda \approx 11$ μm and liquid water content, and between absorption at $\lambda \approx 3.8$, 9.5 μm and liquid water content in fog has several practical applications. For example, for a fog with liquid water content $W = 0.1$ g m^{-3} we predict extinction and absorption coefficients of $\sigma_e(\lambda = 11\ \mu\text{m}) = 13$ km^{-1}, $\sigma_a(3.8\ \mu\text{m}) = 1.8$ km^{-1}, $\sigma_a(5.3\ \mu\text{m}) = 3.1$ km^{-1} and $\sigma_a(9.5\ \mu\text{m}) = 5.7$ km^{-1}. Integrated liquid water content along a path in fog and haze could be inferred from a CO_2 laser ($\lambda = 10.6$ μm) transmissometer measurement according to (1). Of course the path must be short enough that multiple-scattering effects and forward-scattering corrections (Deepak and Box, 1978) are negligible. Carlon *et al.* (1977) previously realized this application for a transmission measurement at $\lambda = 12.5$ μm. An application of the σ_a–W relationship is that liquid water content of fog at a particular point could be determined by measurement of fog droplet absorption in the spectral region $\lambda \approx 3.8$, 9.5 μm according to Eq. (7). The spectrophone technique has been demonstrated to be suitable for *in situ* measurement of particulate absorption by Bruce and Pinnick (1977), so that measurement of fog droplet absorption with either a CO_2 laser spectrophone tuned to a wavelength $\lambda \approx 9.5$ μm, or a DF laser spectrophone ($\lambda \approx 3.8$ μm) could be used to infer fog liquid water content. Of course the spectrophone measurement of absorption could also be used to infer fog extinction at $\lambda \approx 11$ μm. The Eq. (7) relation between fog absorption and liquid water content might also be used in calculation of fog emissivities.

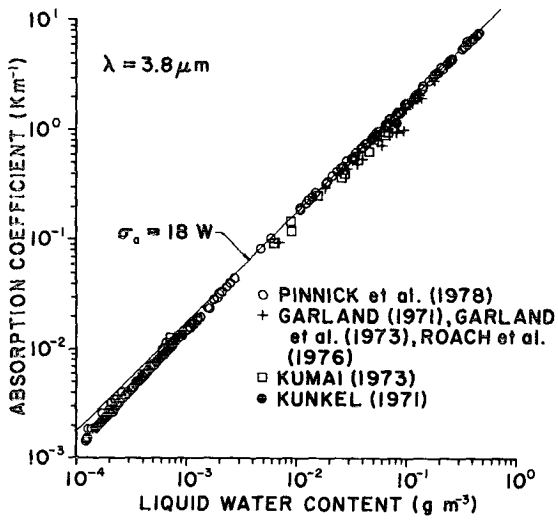

FIG. 8. Variation of absorption coefficient with liquid water content in atmospheric fog and haze for 341 size distribution measurements made at different geographic locales and under a variety of meteorological conditions. In the infrared region around $\lambda = 3.8$ μm there exists a linear, size-distribution-independent relation between the volume absorption coefficient σ_a and the liquid water content W of the form of Eq. (7). Consequently, the results of all measurements are close to a straight line. The predicted relation between absorption σ_a and liquid water content W according to Eq. (7) is shown by the straight line.

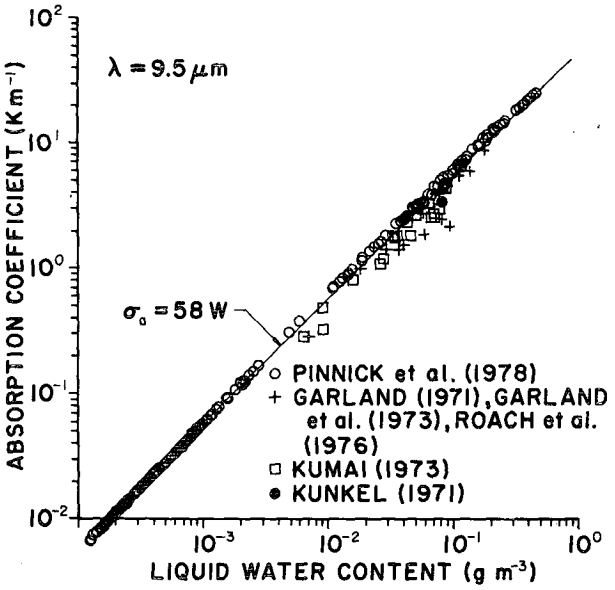

FIG. 9. As in Fig. 8 except for $\lambda = 9.5$ μm.

6. Conclusions

Chýlek's (1978) prediction of a linear relation, independent of the form of the size distribution, between extinction at $\lambda \approx 11$ μm and liquid water content of fog has been verified within a factor 2 for 341 different fog and haze droplet distributions

measured under a variety of meteorological conditions. The prediction generally works better for radiation fogs than advection fogs. A similar linear relation between fog droplet absorption at $\lambda \approx 3.8$, 9.5 μm and liquid water content has been derived and validated using the same 341 distributions. However, there exists no size-distribution-independent relation between extinction in the visible ($\lambda = 0.55$ μm) and fog liquid water content. Three practical applications of these findings are suggested: 1) inference of fog-integrated liquid water content along a path by measurement of laser transmission (at $\lambda \approx 11$ μm) along that path; 2) inference of fog liquid water content at a particular point from measurement of fog droplet absorption with a DF or CO_2 laser spectrophone; and 3) calculation of fog emissivities in the infrared from knowledge of fog liquid water content.

Acknowledgment. We gratefully acknowledge John A. Garland, Environmental and Medical Sciences Division, Harwell, who supplied his raw data of fog size distributions. One of us (P.C.) was partially supported by a grant from the U.S. Army Research Office. On request the authors will send to interested researchers a more detailed report of this work.

REFERENCES

Arnulf, A., J. Bricard, E. Curé and C. Véret, 1957: Transmission by haze and fog in the spectral region 0.35 to 10 microns. *J. Opt. Soc. Amer.*, **47**, 491–498.

Bruce, C. W., and R. G. Pinnick, 1977: In situ measurements of aerosol absorption with a resonant CW laser spectrophone. *Appl. Opt.*, **16**, 1762–1765.

Carlon, H. R., D. Anderson, M. Milham, T. Tarnove and R. Frickel, 1977: Infrared extinction spectra of some common liquid aerosols. *Appl. Opt.*, **16**, 1598–1605.

Chýlek, Petr, 1978: Extinction and liquid water content of fogs. *J. Atmos. Sci.*, **35**, 296–300.

Deepak, Adarsh, and M. A. Box, 1978: Forward scatting corrections for optical extinction measurements in aerosol media. 2: Polydispersions. *Appl. Opt.*, **17**, 3169–3176.

Eldridge, R. G., 1961: A few fog drop-size distributions. *J. Appl. Meteor.*, **18**, 671–676.

——, 1966: Haze and fog aerosol distributions. *J. Atmos. Sci.*, **23**, 605–613.

——, 1971: The relationship between visibility and liquid water content in fog. *J. Atmos. Sci.*, **28**, 1183–1186.

Garland, J. A., 1971: Some fog droplet size distributions obtained by an impaction method. *Quart. J. Roy. Meteor. Soc.*, **97**, 483–494.

——, J. R. Branson and L. C. Cox, 1973: A study of the contribution of pollution to visibility in a radiation fog. *Atmos. Environ.*, **7**, 1079–1092.

Hale, G., M., and M. R. Querry, 1973: Optical constants of water in the 200 nm to 20 μm wavelength region. *Appl. Opt.*, **12**, 555–563.

Hänel, G., 1976: The properties of atmospheric aerosol particles as functions of relative humidity at thermodynamic equilibrium with the surrounding moist air. *Advances in Geophysics*, Vol. 19, Academic Press, 73–188.

——, and K. Bullrich, 1978: Physico—chemical property models of tropospheric aerosol particles. *Beitr. Phys. Atmos.*, **51**, 129–138.

Kumai, Motoi, 1973: Arctic fog droplet size distribution and its effect on light attenuation. *J. Atmos. Sci.*, **30**, 635–643.

Kunkel, B. A., 1971: Fog drop-size distributions measured with a laser hologram camera. *J. Appl. Meteor.*, **10**, 482–486.

May, K. R., 1945: The cascade impactor: An instrument for sampling aerosols. *J. Sci. Instrum.*, **22**, 187–195.

——, 1961: Fog droplet sampling using a modified impactor technique. *Quart. J. Roy. Meteor. Soc.*, **87**, 535–548.

Pinnick, R. G., D. L. Hoihjelle, G. Fernandez, E. B. Stenmark, J. D. Lindberg, S. G. Jennings and G. B. Hoidale, 1978: Vertical structure in atmospheric fog and haze and its effects on IR and visible extinction. *J. Atmos. Sci.*, **35**, 2020–2032.

Pilié, R. J., E. J. Mack, K. C. Kocmond, W. J. Eadie and C. W. Rogers, 1975: The life cycle of valley fog. Part II: Fog microphysics. *J. Appl. Meteor.*, **14**, 364–374.

Platt, C. M. R., 1976: Infrared absorption and liquid water content in stratocumulus clouds. *Quart. J. Roy. Meteor. Soc.*, **102**, 553–561.

Roach, W. T., R. Brown, S. J. Caughey, J. A. Garland and C. J. Readings, 1976: The physics of radiation fog: I—a field study. *Quart. J. Roy. Meteor. Soc.*, **102**, 313–333.